Fast Hue and Range Preserving Histogram Specification: Theory and New Algorithms for Color Image Enhancement

Mila Nikolova (Senior Member IEEE), and Gabriele Steidl

***Abstract*—Color image enhancement is a complex and challenging task in digital imaging with abundant applications. Preserving the hue of the input image is crucial in a wide range of situations. We propose simple image enhancement algorithms which conserve the hue and preserve the range (gamut) of the R, G, B channels in an optimal way. In our setup, the intensity input image is transformed into a target intensity image whose histogram matches a specified, well-behaved histogram. We derive a new color assignment methodology where the resulting enhanced image fits the target intensity image. We analyse the obtained algorithms in terms of chromaticity improvement and compare them with the unique and quite popular histogram based hue and range preserving algorithm of Naik and Murthy. Numerical tests confirm our theoretical results and show that our algorithms perform much better than the Naik-Murthy algorithm. In spite of their simplicity, they compete with well-established alternative methods for images where hue-preservation is desired.**

***Index Terms*—color image enhancement, scaling and shifting methods, hue preservation, gamut problem, exact histogram specification, color perception.**

I. Introduction

This paper assists to the tremendous progress in digital color imaging and display technology. In spite of the important amount of research, color perception and color appearance are still open problems. The demand for fast efficient algorithms improving the color content of digital images has increased dramatically. The applications of color image improvement are abundant. They concern for example digital cameras and mobile phone cameras, medical imaging, video, post-production industry, restoration of old pictures and movies.

Typically, color images are stored and viewed using three components (channels): red (R), green (G) and blue (B). In this paper we aim to design color image enhancement methods in the RGB space sharing three important features, namely *hue and range (gamut) preservation* and *low computational complexity*. The hue describes in each area of an image the dominant color ingredient that one really perceives, e.g., red, orange, magenta, yellow and so on [1], [2]. The hue has the nice property of being invariant under changes of direction and intensity of the incident light [3]. Thus, by preserving the hue and enhancing the brightness, the obtained image will appear more colorful. Examples where the hue is modified are shown in Fig. 1. *The range (gamut) preservation* is often omitted in works on image enhancement; see, e.g. the recent textbook [2, p. 80]. Each color channel in a digital image can only take a limited number, say L, of integer values, e.g., $L = 256$ for 8-bit coding. If the enhancement method produces larger or smaller values these are clipped back to the boundary of $[0, L-1]$ which also changes the hue. In Fig. 1 right 36.1 % of the pixels are clipped back to 255 which yields too many yellow pixels. Finally, a *low computational complexity* of algorithms is particularly important when dealing with "megapixel" images taken by commercial cameras, resources in hardware implementations and extensions to video.

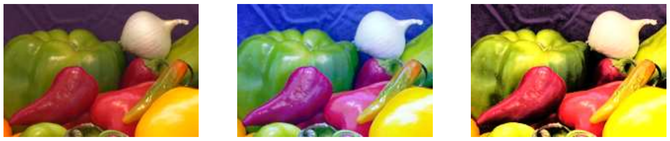

Fig. 1. Histogram equalization (HE). Left: Original image *onion* (Matlab IPT image credits notice). Middle: HE to each color channel independently. Right: Enhancement in three steps following [2]: RGB to HSI transform, HE of the intensity channel, then HSI to RGB transform. Here 36.1 % of the pixels have values in $(255, 443.5]$.

Remark 1. *Fully automatic color image enhancement faces (at least) two major limits: i) "The chemical compounds that form color receptors vary among the population. The physical shapes of the receptors vary among the population and within the retina. Thus, the color vision among observers with normal color vision varies significantly." [1, p. 18]. ii) Image enhancement is always driven by an application: typically the user needs* specific *visual information determined by his/her purpose. Further subjective criteria are of paramount importance [2].*

Consequently, we do not look for *fully* automatic image enhancement algorithms. Here we focus on histogram based methods. The selection of a suitable target histogram enables the user's needs to be satisfied. Moreover we wish to conceive fast algorithms. In order to achieve our goals, we propose simple algorithms composed of two stages:

(a) the intensity channel of the input RGB image is matched to a specified histogram which gives us the target intensity image;
(b) the RGB color values are computed based on the target

M. Nikolova is with CMLA – CNRS, ENS Cachan, 61 av. President Wilson, 94235 Cachan Cedex, France (email: nikolova@cmla.ens-cachan.fr). Her work was supported by the "FMJH Program Gaspard Monge in optimization and operation research", and by the support to this program from EDF.

G. Steidl is with the Dept. of Mathematics, University of Kaiserslautern, 67663 Kaiserslautern, Germany (email: steidl@mathematik.uni-kl.de).

intensity image so that they satisfy the hue and gamut constraints in an optimal way.

These stages are briefly commented below.

Stage (a). Exact histogram specification (HS), also known as histogram matching, of single-valued (gray-valued) images aims to transform an input image to an output image which exactly fits a prescribed target histogram. Histogram equalization (HE) is a particular case of HS where the target histogram is uniform. Usually HE leads to unnatural images and should not be the target of choice. We do not focus on the construction of target histograms. Instead, we adopt a simple approach inspired by [4]. For digital image HS is an ill posed problem [5]. The clue to ensuring exact HS is to obtain a *meaningful total strict ordering* of all pixels in the input digital image. We perform exact HS using the algorithm in [32] which currently provides the best pixel ordering in terms of quality and speed.

Stage (b). The *extension of histogram methods to color images* is a quite complex task. The histogram of a gray-value image is 1-D while the histogram of a color image is 3-D which gives rise to an under-determined problem. For instance, applying HE to each color channel independently changes the color content (the hue) of the image, see Fig. 1 middle. Further it is not easy to produce color images that respect the range constraints; see Fig. 1 right. As a central result of this paper, we propose a general and optimal hue and range preserving color assignment methodology.

Related work. Since the inaugural paper [6] providing *PDE-based and variational formulations* for image histogram modifications, these methods were further expanded to deal with color image enhancement; see, e.g., [7], [8], [9], [10]. These approaches provide flexible tools to incorporate various knowledge on human visual perceptual phenomena, typically in relation with Retinex theory [11]. An automatic color enhancement (ACE) algorithm for digital images, mimicking some characteristics of the human visual system, has been proposed in [12] and refined in [13]. A fast implementation of ACE was developed in [14]. A perceptually inspired variational approach allowing a more flexible control of contrast adjustment and attachment to data was proposed in [7]. A numerical implementation of the gradient descent technique applied to the corresponding energy functionals coincides with the equation of the ACE. Some basic requirements for ”perceptually inspired” objectives were formulated in [8] and gave rise to successful algorithms [8], [15].

Next we summarize the main approaches via *histogram modification* of color images following a chronological order. Since the suitably normalized histogram of an image is also the *empirical* probability distribution of its pixel values, a statistical vocabulary is used in many papers. In [16] a 3-D color histogram in the RGB color space was proposed for HE; the resultant images present an excessive brightness for bright pixels, see [17]. A method that preserves both the hue and the range (gamut) constraints was inaugurated by Naik and Murthy in [18]. Even though this article did not show color image applications, it is a state-of-the-art method applied in many papers; see, e.g., [19], [17]. As to the choice of the color space, some methods work directly in the RGB space while others operate in transformed color spaces, e.g., LHS, HSI, YIQ, HSV, etc., see [5]. When processing is done in a transform color space, coming back to the original RGB space typically generates a gamut problem, as cautioned in [18]. Beyond the additional numerical cost, a post-processing in RGB is then needed (often realized using [18]). Gray-value grouping was tentatively extended to color HE in [20]. In [21], a new definition of the histogram of a color image was introduced whose cumulative distribution function (cdf) is the product of the marginal cdf’s of each color channel. Then the color values are increased / decreased by the same amount iteratively. This work was refined in a later paper [22]. Another approach, developed in [19], is to work in the HSI space where the hue and the saturation are equalized and then processed using probability smoothing. All pixels in the RGB space that present gamut problem are corrected using [18]. A generic brightness preserving dynamic histogram equalization scheme, composed of five steps, was proposed in [23]. This scheme was applied to color images in several ways, including transforms into other color spaces. The work in [17] demonstrates that the methods in [19], [21], [16] based on higher dimensional histogram definition, increase the brightness of the image and cannot fit the prescribed uniform histogram. The main conclusion is that *only the 1-D histogram of the intensity channel can be considered for equalization*. The new color values are then computed using the algorithm in [18]. The method in [17] was recently improved in [24]. In order to avoid the excessive contrast enhancement due to HE, a histogram mixing strategy was applied in [25]. There are also many histogram based techniques where the enhancement function is an S-type, or power, or logarithmic transform; see, e.g., [26], [27], [28], [29]. In particular, the approach in [27] is based on models for color perception and is automatic. Unfortunately, there are no algorithms nor tests on color images.

Contributions. We propose a general affine model for fast hue and range preserving image enhancement in the RGB space which gives rise to Algorithm 3. Two simple but important instances of this algorithm are the Multiplicative algorithm 4 and the Additive algorithm 5. We show how the outcome of Algorithm 3 can be faithfully approximated as a convex combination of the images obtained by Algorithm 4 and Algorithm 5, which is quite practical. The enhancement performances of our algorithms and the Naik-Murthy algorithm [18] are analyzed in terms of their chromaticity improvement. In all cases, our algorithms clearly outperform the algorithm in [18] recently applied to color images in [17]. All numerical tests confirm our theoretical results. Our algorithms are simple and fast. They are really efficient when one wishes to give a better clarity of images (not too altered by artifacts) while preserving the original color ambience.

Outline. In Section II we sketch our HS method and present the Maik-Murthy algorithm [18]. Section III presents our approach for color image enhancement. In Section IV we evaluate our algorithms and the algorithm in [18] analytically in terms of saturation as well as qualitatively. Section V presents numerical results. Conclusions and points for future work are drawn in Section VI.

The proofs of all statements are given in the Appendix.

II. Preliminaries

Let $w = (w_r, w_g, w_b)$ be an RGB image of size $M \times N$, where $w_c \in \{0, \dots, L-1\}$, $c \in \{r, g, b\}$ are its red, green and blue channels, respectively. For 8-bit images we have $L = 256$. We reorder each color channel columnwise into a vector of size $n := MN$ and address the pixels by the index set $\mathbb{I}_n := \{1, \cdots, n\}$.

A. Histogram Specification

The *intensity* of an RGB image w is defined by [5]

$$f(w) := \frac{1}{3}(w_r + w_g + w_b). \tag{1}$$

Then f has $3(L-1)+1$ different values in $\frac{1}{3}\{0, \cdots, 3(L-1)\}$.

Remark 2. *Instead of the intensity f we can also work with other convex combinations of RGB values. E.g., we can use the weights 0.299, 0.587 and 0.114 which are in proportion to the human perception of the RGB channels, see [1], [2].*

We want to find an intensity image $\widehat{f}$ with gray values in $\{0, \dots, L-1\}$ which has a specified (target) histogram $\widehat{h} = (\widehat{h}_1, \dots, \widehat{h}_L)$, i.e., $\widehat{h}[k] := \sharp\{i \in \mathbb{I}_n : \widehat{f}[i] = k-1\}$, $k = 1, \dots, L$, where $\sharp$ stands for cardinality. Such exact HS can almost never be achieved for images with a small number of different values compared to the number of pixels using the classical statistical method based on the cumulative density function, see [5]. Instead we will apply a procedure based on a *meaningful* strict ascending ordering of the pixels in f. Various ordering algorithms for digital images were proposed in the literature, see e.g. [30], [31], [33]. The method in [32], based on [33], provides currently the best way in terms of speed and quality to order the pixels in digital images. The basic idea is to minimize a smoothed ℓ_1-TV functional by simple fixed point iterations with the original image as initialization. After a few iterations the approximate minimizer has entries which differ (up to very few outliers) pairwise from each other while the ordering of the original gray values is retained. Let ∇ denote the discrete gradient operator (horizontal and vertical forward differences), see [32], ∇^{T} its transposed and let

$$\eta(t) := \frac{t}{\alpha + |t|} \quad \text{and} \quad \eta^{-1}(y) = \frac{\alpha y}{1 - |y|}, \tag{2}$$

where $\alpha := 0.05$ is the default value. Note that $\eta = \theta'$ where $\theta(t) := |t| - \alpha \log(1 + \frac{|t|}{\alpha})$, see [32]. Once a strict ordering is obtained, exact HS is direct. Our HS algorithm reads as:

Algorithm 1 HS using strict ordering [32]

```
Initialization: $u^{(0)} := f$, $\beta := 0.1$, target histogram $\widehat{h}$, iteration number $K$ (default $K := 5$), $c_0 := 0$.

1. For $k = 1, \dots, K$ compute
      $u^{(k)} := f - \eta^{-1}\big(\beta \nabla^{\mathrm{T}} \eta(\nabla u^{(k-1)})\big)$.
2. Obtain the ordering $\{i_j\}_{j=1}^n$ of $\mathbb{I}_n$ from the ascending sort of the entries of $u^{(K)}$.
3. For $k = 0, \dots, L-1$ set $c_{k+1} := c_k + h_k$ and
      $\widehat{f}[c_k + 1] = \dots = \widehat{f}[c_{k+1}] = k$.
```

The importance of a meaningful strict ordering for HS is illustrated in Fig. 2 in the context of HE. The Matlab built-in function histeq does not involve a strict ordering of f and the resulting histogram of $\widehat{f}$ is not uniform. This entails some artifacts shown in (a). Such artifacts are not observed in (b) obtained using our Algorithm 1. The colors in Fig. 2(a)-(b) were assigned using Algorithm 2 given in the next subsection.

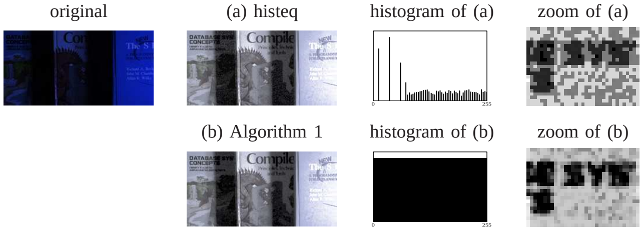

Fig. 2. Illustration of the importance of a meaningful ordering. Top: Original image and application of Matlab histeq. Bottom: Application of Algorithm 1.

B. Hue and Range Preservation

Range preservation is a mandatory constraint for all digital imaging devices [4]. A transformed version $\widehat{w}$ of w can be correctly depicted only if

$$\widehat{w}_c[i] \in [0, L-1] \quad \forall\, i \in \mathbb{I}_n \quad \forall\, c \in \{r,\, g,\, b\}\ , \tag{3}$$

since no more than L digits can be displayed. Otherwise, the obtained image is modified according to the visualization device - which is quite an ad-hoc option; see e.g., Fig. 1 right.

The *hue* of an image w is given by $H(w) = 0$ if $w_r = w_g = w_b$ and otherwise by

$$H(w) := \begin{cases} \theta & \text{if } w_b \le w_g, \\ 360^o - \theta & \text{if } w_b > w_g, \end{cases} \tag{4}$$

where

$$\theta := \arccos \frac{\frac{1}{2}((w_r - w_g) + (w_r - w_b))}{((w_r - w_g)^2 + (w_r - w_b)(w_g - w_b))^{\frac{1}{2}}},$$

see [5]. Note that the denominator of θ can be rewritten as $(\frac{1}{2}((w_r - w_g)^2 + (w_r - w_b)^2 + (w_g - w_b)^2))^{\frac{1}{2}}$.

Remark 3. *The simplest hue and range preserving method is to apply the same affine mapping $\xi(w) := aw + b$ to all pixels, computing a and b so that the least and the largest pixels in $\xi(w)$ are 0 and $L-1$, respectively. Let $w_{\max} := \max\{w_c[i]; c \in \{r,\, g,\, b\},\, i \in \mathbb{I}_n\}$ and let $w_{\min} := \min\{w_c[i]; c \in \{r,\, g,\, b\},\, i \in \mathbb{I}_n\}$. Then $\xi(w)$ given by*

$$\xi(w) := (L-1)\frac{w - w_{\min}}{w_{\max} - w_{\min}} \tag{5}$$

is the desired stretching of w. For example, see Fig. 16, top.

It is easy to see that the hue of the modified image $\widehat{w}$ is also preserved if the color values of *each* pixel are modified by the same affine transform

$$\widehat{w}_c[i] = a[i] w_c[i] + b[i], \quad c \in \{r,\, g,\, b\}, \tag{6}$$

where the constants $a[i]$ and $b[i]$ have to be chosen for any $i \in \mathbb{I}_n$. Finding other appropriate hue-preserving transforms is an interesting problem. For $a[i] = 1$, model (6) amounts to an *additive transform*, usually called *shifting*. For $b[i] = 0$, it is a *linear/multiplicative* transform known as *scaling*. Both scaling and shifting have been introduced in [34], [35]. In general, the result of (6) fails the range constraint (3).

The gamut problem was examined by Naik and Murthy in [18] in the scaling case for $a[i] = \widehat{f}[i]/f[i]$, where $\widehat{f}$ is a target intensity. If $\widehat{f}[i]/f[i] > 1$, the range constraint (3) *might* not be guaranteed. In such a case the authors propose to avoid the *potential* problem by switching from the RGB color space to the CMY (Cyan $= L-1-$R, Magenta $= L-1-$G, Yellow $= L-1-$B) space and then to transform back into RGB. This correction step reads for all $c \in \{r, g, b\}$ as

$$\widehat{w}_c[i] = L - 1 - \frac{L-1-\widehat{f}[i]}{L-1-f[i]}(L-1-w_c[i]) \quad \text{if} \quad \frac{\widehat{f}[i]}{f[i]} > 1.$$

This formula is equivalent to $\widehat{w}_c[i] = \frac{L-1-\widehat{f}[i]}{L-1-f[i]}(w_c[i] - f[i]) + \widehat{f}[i]$, so that the algorithm in [18] can be formulated as follows:

Algorithm 2 Naik and Murthy [18]

```
1. Compute the intensity $f$ of $w$ and the target intensity $\widehat{f}$.
2. For $i \in \mathbb{I}_n$ compute
    (i)  $\widehat{w}_c[i] := \frac{\widehat{f}[i]}{f[i]} w_c[i]$    if $\frac{\widehat{f}[i]}{f[i]} \le 1$
    (ii) $\widehat{w}_c[i] := \frac{L-1-\widehat{f}[i]}{L-1-f[i]}(w_c[i] - f[i]) + \widehat{f}[i]$    if $\frac{\widehat{f}[i]}{f[i]} > 1$
```

Algorithm 2 is often used to avoid the gamut problem.

III. New Affine Histogram Specification Models

In this section we develop our affine color enhancement methodology. Given an RGB image w and a target histogram, we compute its intensity f by (1) and then the target intensity image $\widehat{f}$ by Algorithm 1. Our next goal is to transform w into an image $\widehat{w}$ having the following properties:

(a) Intensity fit: $\widehat{f} = \frac{1}{3}(\widehat{w}_r + \widehat{w}_g + \widehat{w}_b)$.
(b) Hue preservation: the hue of $\widehat{w}$ and w coincide.
(c) Range preservation: $0 \le \widehat{w}_c \le L-1$, $c \in \{r, g, b\}$.

We adopt the hue preserving affine transform (6). Summing up over c in (6) shows that property (a) holds if and only if

$$\widehat{f}[i] = a[i]f[i] + b[i] \quad \Leftrightarrow \quad b[i] = \widehat{f}[i] - a[i]f[i]. \tag{7}$$

Therefore the affine model (6) obeys (a) if and only if

$$\widehat{w}_c[i] = a[i](w_c[i] - f[i]) + \widehat{f}[i], \quad c \in \{r, g, b\}. \tag{8}$$

Two particular instances of (6) are the following:

– *Scaling*: For $b[i] = 0$, model (8) reads as

$$\widehat{w}_c[i] = \frac{\widehat{f}[i]}{f[i]} w_c[i], \quad c \in \{r, g, b\}. \tag{9}$$

– *Shifting*: For $a[i] = 1$, model (8) becomes

$$\widehat{w}_c[i] = w_c[i] - f[i] + \widehat{f}[i], \quad c \in \{r, g, b\}.$$

We have to adapt these models so that they preserve the range. We will use for all $i \in \mathbb{I}_n$ the magnitudes

$$\begin{aligned} M[i] &:= \max\{w_c[i] : c \in \{r, g, b\}\}, \\ m[i] &:= \min\{w_c[i] : c \in \{r, g, b\}\} \end{aligned} \tag{10}$$

and similarly $\widehat{M}[i]$ for the maximum and $\widehat{m}[i]$ for the minimum of the RGB components of $\widehat{w}[i]$ given in (8).

Remark 4. *By the definitions of f, m and M we have*

$$0 \le m[i] \le f[i] \le M[i] \le L-1.$$

Further $M[i] = f[i]$, resp., $m[i] = f[i]$ if and only if $w_r[i] = w_g[i] = w_b[i]$, i.e., $w[i]$ is a gray pixel.

A pixel $\widehat{w}[i]$ has an *upper gamut* problem if $\widehat{M}[i] > L-1$ and a *lower gamut* problem if $\widehat{m}[i] < 0$. We will treat these gamut problems in an optimal way in the following sense:

- Assume that we have an upper gamut problem, i.e., $\widehat{M}[i] > L-1$ for some $i \in \mathbb{I}_n$. Then $\widehat{M}[i] = \widehat{w}_k[i]$ for some $k \in \{r, g, b\}$ and the best correction of this pixels is clearly to choose $a[i]$ in (8) so that $\widehat{w}_k[i]$ has the closest value in the range, i.e. $\widehat{w}_k[i] = L-1$, see, e.g., [4]. Equivalently,

$$L - 1 = a[i](M[i] - f[i]) + \widehat{f}[i]. \tag{11}$$

From Remark 4 we know that for non gray-valued pixels $M[i] - f[i] > 0$, so that

$$a[i] = \frac{L-1-\widehat{f}[i]}{M[i] - f[i]} \ge 0.$$

Thus, for the upper gamut problem, the corrected color values of pixel i are given by

$$\widehat{w}_c[i] = \frac{L-1-\widehat{f}[i]}{M[i]-f[i]}(w_c[i] - f[i]) + \widehat{f}[i], \quad c \in \{r, g, b\}. \tag{12}$$

- Assume we have a lower gamut problem $\widehat{m}[i] < 0$ for some $i \in \mathbb{I}_n$. Let $k \in \{r, g, b\}$ be such that $\widehat{w}_k[i] = \widehat{m}[i]$. Then the optimal correction in (8) obeying (c) is to set $\widehat{w}_k[i] = 0$, i.e.,

$$0 = a[i]\ (m[i] - f[i]) + \widehat{f}[i]. \tag{13}$$

By Remark 4 $f[i] - m[i] > 0$ for non gray pixels, so that

$$a[i] = \frac{\widehat{f}[i]}{f[i] - m[i]} \ge 0.$$

Hence for the lower gamut problem, the corrected color value at i is given by

$$\widehat{w}_c[i] = \frac{\widehat{f}[i]}{f[i]-m[i]}(w_c[i] - f[i]) + \widehat{f}[i], \quad c \in \{r, g, b\}. \tag{14}$$

A. Affine Algorithm with Optimal Range Preservation

Our affine model is a convex combination of the shifting and scaling models for some $\lambda \in [0, 1]$:

$$\begin{aligned} \widehat{w}_c[i] &= \lambda \frac{\widehat{f}[i]}{f[i]} w_c[i] + (1-\lambda)\left(w_c[i] - f[i] + \widehat{f}[i]\right) \qquad (15) \\ &= a[i](w_c[i] - f[i]) + \widehat{f}[i], \end{aligned}$$

where

$$a[i] := \lambda \frac{\widehat{f}[i]}{f[i]} + 1 - \lambda \tag{16}$$

with upper and lower gamut corrections (12) and (14) if necessary. Clearly, for $\lambda = 1$ we have the scaling model and for $\lambda = 0$ the shifting one. Algorithm 2 corresponds to $\lambda = 1$ in (15) but the gamut problem is tackled just by thresholding $a[i]$ at one; this appears to be an important drawback.

The next propositions show that correcting the gamut problems using (12) or (14) does not yield new gamut problems.

Proposition 1. *Assume that pixel $i \in \mathbb{I}_n$ in* (15) *has an upper gamut problem. Then its correction $\widehat{w}_c[i]$ in* (12) *satisfies*

$$0 \le \widehat{w}_c[i] \le L - 1, \quad c \in \{r,\, g,\, b\}.$$

Let us mention that a lower gamut problem can obviously not appear for the multiplicative model (9) i.e. for $\lambda = 1$.

Proposition 2. *Let $\lambda \in [0, 1)$. Assume that pixel $i \in \mathbb{I}_n$ in* (15) *has an lower gamut problem. Then its correction $\widehat{w}_c[i]$ in* (14) *satisfies*

$$0 \le \widehat{w}_c[i] \le L - 1, \quad c \in \{r,\, g,\, b\}.$$

Using Propositions 1 and 2, the optimal range-preserving approximation of our affine model (15) can be computed in one iteration where all pixels in the input image are modified only once. The algorithm is described below.

Algorithm 3 Optimal Range-Preserving Enhancement

```
1. Compute the intensity $f$ of $w$ by (1) and the target intensity $\widehat{f}$ using Algorithm 1 for given $\widehat{h}$.
2. For $i \in \mathbb{I}_n$ compute $M[i]$ and $m[i]$ by (10). If $f[i] = 0$, then $\widehat{w}[i] := 0$. Otherwise compute
       $a[i] := \lambda \frac{\widehat{f}[i]}{f[i]} + (1 - \lambda),$
       $G_m^\lambda[i] := a[i](m[i] - f[i]) + \widehat{f}[i],$
       $G_M^\lambda[i] := a[i](M[i] - f[i]) + \widehat{f}[i]$
   and for all $c \in \{r,\, g,\, b\}$:
    (i)  $\widehat{w}_c[i] := a[i]\,(w_c[i] - f[i]) + \widehat{f}[i]$
         if $G_m^\lambda[i] \ge 0$ and $G_M^\lambda[i] \le L - 1$ ,
   (ii)  $\widehat{w}_c[i] := \frac{L-1-\widehat{f}[i]}{M[i]-f[i]}(w_c[i] - f[i]) + \widehat{f}[i]$
         if $G_M^\lambda[i] > L - 1$,
  (iii)  $\widehat{w}_c[i] := \frac{\widehat{f}[i]}{f[i]-m[i]}(w_c[i] - f[i]) + \widehat{f}[i]$
         if $G_m^\lambda[i] < 0$.
```

Algorithm 3 and the role of λ is illustrated in Fig. 3. The images were computed for Gaussian target histogram with parameters $(l, r) = (0.9, 0.1)$, see (27), Sec. V-A.

B. Multiplicative, Additive Algorithms and their Combinations

For $\lambda \in \{0, 1\}$ Algorithm 3 yields two simple range preserving scaling and shifting algorithms called Multiplicative and Additive algorithm, respectively. Observing that

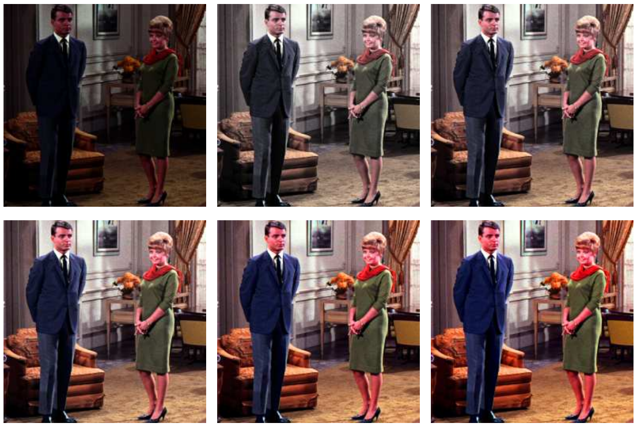

Fig. 3. Input image *couple* (top left) and its enhancement by our Algorithm 3 for $\lambda = 0,\ \frac{1}{4},\ \frac{1}{2},\ \frac{3}{4},\ 1$. Here the size of the sets $\mathcal{U}(\lambda)$ in (18) in percent of all image pixels are $0.70,\ 1.24,\ 2.12,\ 3.13,\ 4.17$ and the sets $\mathcal{L}(\lambda)$ are empty. All nuances between the very colorful image $\widehat{w}^\times$ and the grayish image $\widehat{w}^+$ can be also obtained by their convex combinations in (17).

$$\begin{aligned} G_m^0[i] &= m[i] - f[i] + \widehat{f}[i], \\ G_M^0[i] &= M[i] - f[i] + \widehat{f}[i], \\ G_M^1[i] &= \tfrac{\widehat{f}[i]}{f[i]} M[i] \end{aligned}$$

these algorithms read as follows:

Algorithm 4 Multiplicative Color Enhancement

```
1. Compute the intensity $f$ of $w$ and the target intensity $\widehat{f}$ using Algorithm 1.
2. For $i \in \mathbb{I}_n$ compute $M[i]$ by (10). If $f[i] = 0$, then $\widehat{w}[i] := 0$. Otherwise compute
     $G_M^1[i] = \frac{\widehat{f}[i]}{f[i]} M[i]$
   and for all $c \in \{r,\, g,\, b\}$:
    (i)  $\widehat{w}_c[i] := \frac{\widehat{f}[i]}{f[i]}\, w_c[i]$
         if $G_M^1[i] \le L - 1$,
   (ii)  $\widehat{w}_c[i] := \frac{L-1-\widehat{f}[i]}{M[i]-f[i]}(w_c[i] - f[i]) + \widehat{f}[i]$
         if $G_M^1[i] > L - 1$.
```

Algorithm 5 Additive Color Enhancement

```
1. Compute the intensity $f$ of $w$ and the target intensity $\widehat{f}$ using Algorithm 1.
2. For $i \in \mathbb{I}_n$ compute $M[i]$ and $m[i]$ by (10). If $f[i] = 0$, then $\widehat{w}[i] := 0$. Otherwise compute
   $G_m^0[i] = m[i] - f[i] + \widehat{f}[i]$ and $G_M^0[i] = M[i] - f[i] + \widehat{f}[i]$
   and for all $c \in \{r,\, g,\, b\}$:
    (i)  $\widehat{w}_c[i] := w_c[i] - f[i] + \widehat{f}[i]$
         if $G_m^0[i] \ge 0$  and  $G_M^0[i] \le L - 1$,
   (ii)  $\widehat{w}_c[i] := \frac{L-1-\widehat{f}[i]}{M[i]-f[i]}(w_c[i] - f[i]) + \widehat{f}[i]$
         if $G_M^0[i] > L - 1$,
   (ii)  $\widehat{w}_c[i] := \frac{\widehat{f}[i]}{f[i]-m[i]}(w_c[i] - f[i]) + \widehat{f}[i]$
         if $G_m^0[i] < 0$.
```

Let $\widehat{w}^{\times}$ be obtained by the Multiplicative algorithm 4 and $\widehat{w}^{+}$ by the Additive algorithm 4. For some $\lambda \in [0,1]$, consider

$$\widetilde{w}_c := \lambda \widehat{w}_c^{\times} + (1-\lambda)\widehat{w}_c^{+} \quad \forall c \in \{r,\, g,\, b\}. \tag{17}$$

Since $\widetilde{w}_c$ is a convex combination of $\widehat{w}^{\times}$ and $\widehat{w}^{+}$, it obeys all conditions (a)-(c). We want to know if $\widetilde{w}_c$ can replace the affine Algorithm 3. In order to answer this question, we set

$$\begin{aligned} \mathcal{U}(\lambda) &:= \{i \in \mathbb{I}_n : G_M^{\lambda}[i] > L-1\}, \\ \mathcal{L}(\lambda) &:= \{i \in \mathbb{I}_n : G_m^{\lambda}[i] < 0\}. \end{aligned} \tag{18}$$

Here $\mathcal{U}(\lambda)$ corresponds to the upper gamut step (ii) and $\mathcal{L}(\lambda)$ – to the lower gamut step (iii) in Algorithm 3.

Proposition 3. *The sets $\mathcal{U}(\lambda)$ and $\mathcal{L}(\lambda)$ defined in* (18) *fulfill $\mathcal{L}(1) = \varnothing$ and*

$$\mathcal{U}(\lambda_1) \subseteq \mathcal{U}(\lambda_2), \quad \mathcal{L}(\lambda_1) \supseteq \mathcal{L}(\lambda_2), \quad 0 \le \lambda_1 < \lambda_2 \le 1.$$

In particular, (18) yields

$$\begin{aligned} \mathcal{U}(1) &= \left\{ i \in \mathbb{I}_n : \tfrac{\widehat{f}[i]}{f[i]} M[i] > L-1 \right\}, \\ \mathcal{U}(0) &= \left\{ i \in \mathbb{I}_n : \widehat{f}[i] - f[i] + M[i] > L-1 \right\}, \\ \mathcal{L}(0) &= \left\{ i \in \mathbb{I}_n : \widehat{f}[i] - f[i] + m[i] < 0 \right\}. \end{aligned} \tag{19}$$

From Proposition 3 one has $\mathcal{U}(0) \subseteq \mathcal{U}(1)$. The notation in (19) enables Algorithms 4 and 5 to be restated as follows:
– Multiplicative algorithm $(\lambda = 1)$

$$\begin{aligned} &\text{(i)} \quad \widehat{w}_c[i] = \tfrac{\widehat{f}[i]}{f[i]} \left(w_c[i] - f[i]\right) + \widehat{f}[i] \ \text{ if } i \in \mathbb{I}_n \setminus \mathcal{U}(1), \\ &\text{(ii)} \quad \widehat{w}_c[i] = \tfrac{L-1-\widehat{f}[i]}{M[i]-f[i]} (w_c[i] - f[i]) + \widehat{f}[i] \ \text{ if } i \in \mathcal{U}(1). \end{aligned} \tag{20}$$

– Additive algorithm $(\lambda = 0)$

$$\begin{aligned} &\text{(i)} \quad \widehat{w}_c[i] = (w_c[i] - f[i]) + \widehat{f}[i] \ \text{ if } i \in \mathbb{I}_n \setminus \{\mathcal{U}(0) \cup \mathcal{L}(0)\}, \\ &\text{(ii)} \quad \widehat{w}_c[i] = \tfrac{L-1-\widehat{f}[i]}{M[i]-f[i]} (w_c[i] - f[i]) + \widehat{f}[i] \text{ if } i \in \mathcal{U}(0), \\ &\text{(iii)} \quad \widehat{w}_c[i] = \tfrac{\widehat{f}[i]}{f[i]-m[i]} (w_c[i] - f[i]) + \widehat{f}[i] \text{ if } i \in \mathcal{L}(0). \end{aligned} \tag{21}$$

The relation between $\widetilde{w}_c$ in (17) and the outcome $\widehat{w}$ of Algorithm 3 for the same λ is described in the next proposition.

Proposition 4. *Let $\widehat{w}$ be obtained by Algorithm 3 and $\widetilde{w}$ by* (17) *for the same $\lambda \in [0,1]$. Then it holds for $i \in \mathbb{I}_n \setminus \big\{\mathcal{U}(1) \setminus \mathcal{U}(0) \cup \mathcal{L}(0)\big\}$ that $\widetilde{w}_c[i] = \widehat{w}_c[i]$.*

The sets $\mathcal{U}(1)$, $\mathcal{U}(0)$ and $\mathcal{L}(0)$ are usually small for reasonable target intensity images $\widehat{f}$ (see Table I) and $\mathcal{U}(1) \setminus \mathcal{U}(0)$ contains generally much less pixels than $\mathcal{U}(1)$. If we wish to see the enhancement results $\widehat{w}$ of Algorithm 3 for various $\lambda \in [0,1]$, Proposition 4 justifies to compute instead $\widetilde{w}$ by (17) which is much more practical. Thus, by sliding λ in (17), we can easily move between the two models.

IV. Comparison of the algorithms

A. Saturation Properties

Here we analyze the saturation of images enhanced by our methods and by the Naik-Murthy algorithm. The *saturation* of an RGB image w in the HSI model [5] is defined by

$$S(w) := \begin{cases} 1 - \dfrac{\min\{w_r, w_g, w_b\}}{f(w)} & \text{if } f(w) > 0, \\ 0 & \text{if } f(w) = 0\ . \end{cases} \tag{22}$$

Proposition 5. *Let $S(w[i])$ and $S(\widehat{w}[i])$ denote the saturation of pixel i in the input image w and the image $\widehat{w}$ obtained by our Algorithm 3, respectively. If $f[i] \in \{m[i], M[i]\}$ we have $S(\widehat{w}[i]) = 0$. Otherwise the obtained saturation is given by*

(i) $S(\widehat{w}[i]) = S(w[i]) \left(\lambda + (1-\lambda)\frac{f[i]}{\widehat{f}[i]}\right)$
if $i \in \mathbb{I}_n \setminus \{\mathcal{U}(\lambda) \cup \mathcal{L}(\lambda)\}$,

(ii) $S(\widehat{w}[i]) = S(w[i]) \frac{f[i]}{\widehat{f}[i]} \frac{L-1-\widehat{f}[i]}{M[i]-f[i]}$ *if $i \in \mathcal{U}(\lambda)$,*

(iii) $S(\widehat{w}[i]) = 1$ *if $i \in \mathcal{L}(\lambda)$.*

To clarify the comparison, all magnitudes relevant to Algorithm 2 (Naik and Murthy) hold the superscript $\bullet$, those relevant to Algorithms 4 (Multiplicative) and 5 (Additive) have the superscripts $\times$ and $+$, respectively. In particular, we obtain:
– Algorithm 4 (Multiplicative)

$$\begin{aligned} &\text{(i)} \quad S(\widehat{w}^{\times}[i]) = S(w[i]) && \text{if} \quad i \in \mathbb{I}_n \setminus \mathcal{U}(1), \\ &\text{(ii)} \quad S(\widehat{w}^{\times}[i]) = S(w[i]) \tfrac{f[i]}{\widehat{f}[i]} \tfrac{L-1-\widehat{f}[i]}{M[i]-f[i]} && \text{if} \quad i \in \mathcal{U}(1). \end{aligned} \tag{23}$$

– Algorithm 5 (Additive)

$$\begin{aligned} &\text{(i)} \quad S(\widehat{w}^{+}[i]) = S(w[i]) \tfrac{f[i]}{\widehat{f}[i]} && \text{if} \quad i \in \mathbb{I}_n \setminus (\mathcal{U}(0) \cup \mathcal{L}(0)), \\ &\text{(ii)} \quad S(\widehat{w}^{+}[i]) = S(\widehat{w}^{\times}[i]) && \text{if} \quad i \in \mathcal{U}(0), \\ &\text{(iii)} \quad S(\widehat{w}^{+}[i]) = 1 && \text{if} \quad i \in \mathcal{L}(0). \end{aligned} \tag{24}$$

Let us denote

$$\mathcal{V} := \left\{ i \in \mathbb{I}_n \ : \ \frac{\widehat{f}[i]}{f[i]} > 1 \right\}. \tag{25}$$

By (19) and Remark 4 we find that if $i \in \mathcal{U}(1)$ then $\frac{\widehat{f}[i]}{f[i]} > \frac{L-1}{M[i]} \ge 1$ and that if $i \in \mathcal{L}(0)$, then $\frac{\widehat{f}[i]}{f[i]} < 1 - \frac{m[i]}{f[i]} < 1$. Hence

$$\mathcal{V} \supseteq \mathcal{U}(1) \quad \text{and} \quad \mathcal{L}(0) \subset \mathbb{I}_n \setminus \mathcal{V}. \tag{26}$$

Using the notation in (25), case (i) in Algorithm 2 (Naik-Murthy) holds for any $i \in \mathbb{I}_n \setminus \mathcal{V}$ and step (ii) holds for any $i \in \mathcal{V}$. The saturation of images enhanced by applying the Naik - Murthy Algorithm 2 is given by the following proposition.

Proposition 6. *Let $S(w[i])$ and $S(\widehat{w}^{\bullet}[i])$ denote the saturation of pixel i in the input image w and the image $\widehat{w}^{\bullet}$ obtained by the Naik-Murthy Algorithm 2, respectively. Then*

$$\begin{aligned} &\text{(i)} \quad S(\widehat{w}^{\bullet}[i]) = S(w[i]) && \text{if} \quad i \in \mathbb{I}_n \setminus \mathcal{V}, \\ &\text{(ii)} \quad S(\widehat{w}^{\bullet}[i]) = S(w[i]) \tfrac{f[i]}{\widehat{f}[i]} \tfrac{L-1-\widehat{f}[i]}{L-1-f[i]} && \text{if} \quad i \in \mathcal{V}. \end{aligned}$$

Remark 5. *Proposition 3 and* (26) *show that $\mathcal{V} \supseteq \mathcal{U}(1) \supseteq \mathcal{U}(0)$. Note that all these inclusions are almost always strict; see Table I. E.g., in* (26) *we find $\mathcal{U}(1) = \mathcal{V}$ if and only if $M[i] = L-1$ for all $i \in \mathcal{V}$.*

Using Propositions 5 and 6, the saturation that Algorithms 4, 5 and 2 provide can be rigorously compared.

- Let $i \in \mathbb{I}_n \setminus \mathcal{V}$. Then $i \notin \mathcal{U}(1)$ and $i \notin \mathcal{U}(0)$. Hence

$$S(w[i]) = S(\widehat{w}^{\times}[i]) = S(\widehat{w}^{\bullet}[i]) \le S(\widehat{w}^{+}[i]),$$

where the last inequality becomes an equality only for $\widehat{f}[i] = f[i]$. Beyond this case, only the Additive algorithms 5 increases the saturation if $\widehat{f}[i] < f[i]$. But since the output intensity is decreased, the perceived colorfulness of the pixel is decreased.

- Let $i \in \mathcal{V} \setminus \mathcal{U}(1) = \{i \in \mathbb{I}_n : 1 < \frac{\widehat{f}[i]}{f[i]} \leq \frac{L-1}{M[i]}\}$. Then $i \notin (\mathcal{U}(0) \cup \mathcal{L}(0))$ and consequently
$$S(w[i]) = S(\widehat{w}^{\times}[i]) > S(\widehat{w}^{+}[i]) > S(\widehat{w}^{\bullet}[i])$$
and $S(\widehat{w}^{\bullet}[i])$ decreases faster than $S(\widehat{w}^{+}[i])$ when $\widehat{f}[i]$ increases because
$$\frac{S(\widehat{w}^{\bullet}[i])}{S(\widehat{w}^{+}[i])} = \frac{M[i] - f[i]}{L - 1 - f[i]} < 1.$$
- Let $i \in \mathcal{U}(1)$. Then
$$S(w[i]) > S(\widehat{w}^{\times}[i]) \geq S(\widehat{w}^{\bullet}[i]),$$
where the equality is reached if and only if $M[i] = L - 1$. But for most of the pixels one has $M[i] < L - 1$. Further,
$$S(w[i]) > S(\widehat{w}^{+}[i]) \geq S(\widehat{w}^{\bullet}[i]),$$
where the equality holds if and only if $M[i] = L - 1$ and $i \in \mathcal{U}(0)$. So the inequality is strict for most of the pixels.

In all cases, the images enhanced by the Maik-Murthy algorithm have the weakest saturation. On $\mathbb{I}_n \setminus \mathcal{V}$, where the target intensity is less than the input intensity, the Additive algorithm 5 gives a better saturation than the Multiplicative algorithm 4. On $\mathcal{V} \setminus \mathcal{U}(1)$ the Multiplicative algorithm 4 gives rise to a better saturation than the Additive algorithm 5.

B. *Qualitative comparison*

We begin with a simple but instructive example where we apply Algorithms 4, 5 and 2 to two different "images" each composed of one dark and one bright pixel, resp.,
$$w_{\text{dark}} = (25, 48, 32), \quad w_{\text{bright}} = (80, 172, 108)$$
having the same hue but different intensities $f_{\text{dark}} = 35$ and $f_{\text{bright}} = 120$. In Figs. 4 and 5, the input pixels w are shown on the top row, while the next rows detail the results of the algorithms w.r.t. the target intensity $\widehat{f} \in \{0, \ldots, 255\}$ given on the x-axis. By (19) we see that the pixel belongs to $\mathcal{U}(1)$ for $\widehat{f} > \frac{(L-1)f}{M} =: f_{\mathcal{U}(1)}$, to $\mathcal{U}(0)$ for $\widehat{f} > (L - 1) - M + f =: f_{\mathcal{U}(0)}$, to $\mathcal{L}(0)$ for $\widehat{f} < f - m =: f_{\mathcal{L}(0)}$ and to $\mathcal{V}$ for $\widehat{f} > f := f_{\mathcal{V}}$. The corresponding values for our dark and bright image are given in the following table:

	$f_{\mathcal{U}(1)}$	$f_{\mathcal{U}(0)}$	$f_{\mathcal{L}(0)}$	$f_{\mathcal{V}}$
w_{dark}	185.9	242	10	35
w_{bright}	177.9	203	40	120

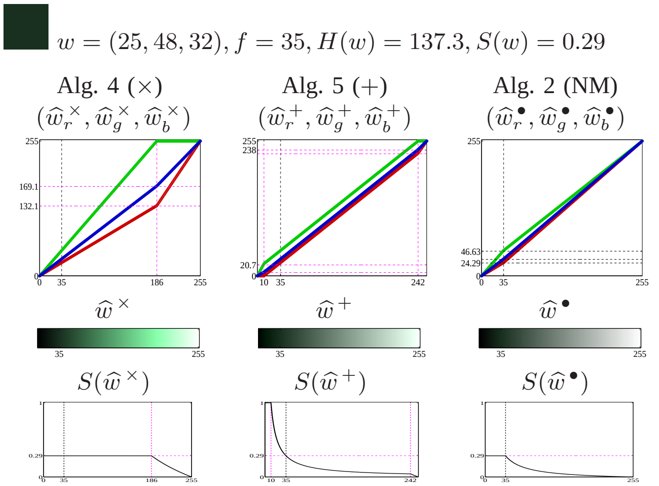

Fig. 4. Enhancement of a quite dark pixel shown in the first row. Second and third rows: the output intensity $\widehat{f}$ is on the x-axis and the plots depict the results of Algorithms 4, 5 and 2. The second row specify the value of each color channel. The third row shows the resulting color $\widehat{w}$ w.r.t. $\widehat{f}$ and the last row plots the saturation of the output pixel as a function of $\widehat{f}$.

Fig. 4 deals with the dark pixel w_{dark}. The Multiplicative algorithm 4 (i) is applied for $\widehat{f} \in [0, 185.9]$. All color values are multiplied by $\widehat{f}/f$, where $\widehat{f}/f > 1$ for $\widehat{f} > 35$ which yields a clear increase of the distance between all color channels. The third row shows a pleasant enhancement of the dark input pixel. By (23) the input saturation is preserved. The Additive Algorithm 5 (i) is performed for $\widehat{f} \in [10,\ 242]$, where all color values are increased by the same amount $\widehat{f} - f$. Since the input pixel is quite dark, the values w_c, $c \in \{r,\, g,\, b\}$ and f are relatively close to each other. For this reason, all color channels $\widehat{w}_c^{+}$ remain close to each other. On $[10,\ 35)$ we have $f > \widehat{f}$ so by (24), $S(\widehat{w}^{+}) > S(w)$ and $S(\widehat{w}^{+})$ continuously decreases from 1 to $S(w) = 0.29$. On $[35,\ 242]$, $S(\widehat{w}^{+})$ decreases from $S(w) = 0.29$ to 0.04 according to $S(w)f/\widehat{f}$. This explains why the colors on the third row remain quite dull, compared to Algorithm 4. For Algorithm 2, case (i) holds only for $\widehat{f} \in [0, 35]$, where the input saturation is preserved. If $\widehat{f} > 35$, step (ii) is performed and $S(\widehat{w}^{\bullet})$ decreases much faster than in Algorithm 5. As a consequence, on $(35, 255]$ the enhanced colors tend to be nearly equal and the obtained color values are nearly gray, see the third row in the figure.

Fig. 5 shows the performance for the brighter pixel w_{bright}. The Multiplicative algorithm 4 (i) is applied for $\widehat{f} \in [0, 177.9]$. The input saturation is preserved. The Additive algorithm 5 (i) holds for $\widehat{f} \in [40, 203]$. On $[40,\ 120]$ the recovered saturation decreases from 1 to $S(w) = 0.33$ and on $(120, 203]$ it slowly decreases to $0.6S(w)$. In Algorithm 2, step (i) holds for $\widehat{f} \leq f = 120$ where the input saturation is unchanged. Step (ii) is applied for $\widehat{f} \in (120, 255]$ – the interval is not so large as in Fig. 4 and the saturation decreases much less fast to zero. On the 3rd row one sees that the colors obtained with all the three algorithms are quite similar.

Remark 6. *From Fig. 4, if a dark pixel has a wrong hue (e.g. due to compression or printing artifacts, noise, color cast, etc.), the Multiplicative algorithm 4 can magnify the intensity of this wrong color. If the input image contains a lot of such pixels, the Additive algorithm 5 can be a better choice.*

Our conclusions drawn in Subsection IV-A and our findings for one pixel images are confirmed by our tests on the two images, *bungalow* (underexposed) and *flower* (slightly lustreless) depicted in Fig. 6 and 7. The distribution of $\widehat{f}[i]/f[i]$ for these two images is very different – the first one ranges on $[0,\ 18]$ and the second one on $[0,\ 1.22]$. Roughly speaking, *bungalow*

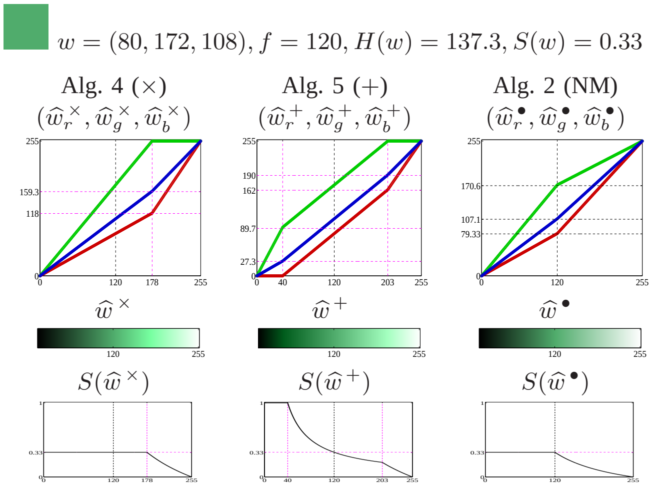

Fig. 5. Enhancement of a quite bright pixel shown in the first row. Arrangement of images as in Fig. 4.

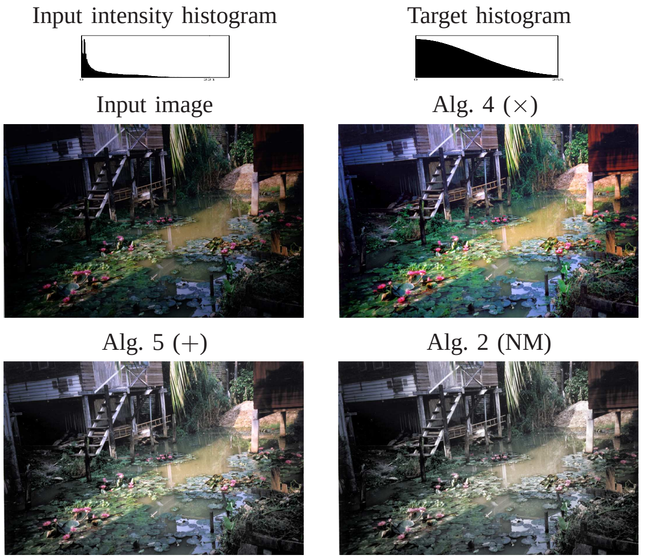

Fig. 6. Original image *bungalow* (660 × 1024) and enhanced versions. For underexposed images the Naik-Murthy algorithm 2 gives nearly gray-valued results. The Multiplicative algorithm 4 gives the most colorful image. The Additive algorithm 5 yields color values between those of the multiplicative and the Naik-Murthy algorithm; it performs better than the last one.

mimics the phenomena explained for Fig. 4 and *flower* those relevant to Fig. 5.

V. Numerical Results

Here we demonstrate the performance of our algorithms to render images where we want to preserve the hue.

A. Target histograms

Our algorithms depend, up to a certain degree, on the choice of a target histogram for the intensity channel. Various target histograms avoiding the drawbacks of HE have been proposed in the literature. Some of them leave gaps in the target histogram which can yeild artifacts as in Fig. 2, see e.g. [20], [26], others preserve the input brightness which limits the enhancement of underexposed images, see, e.g. [23], [28]. The models proposed in [25] combine the input image histogram and a uniform histogram using various penalties and parameters. Instead, we adopt a simple and intuitive approach.

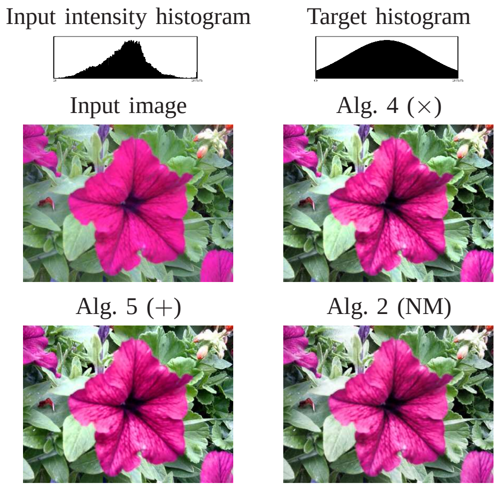

Fig. 7. Original image *flower* (300 × 400) and enhanced versions. All Algorithms 2, 4 and 5 produce very similar results.

A common way for histogram based enhancement is to use the histogram of a well exposed example image; see, e.g., [4]. Commercials in photography and image processing software (e.g., Photoshop) mention that well exposed pictures typically have bell-shaped histograms. Based on these advises we focus on target histograms whose shapes are Gaussian functions $\widehat{h}_{\text{G}}$, with domain $[0, L-1]$, fixed so that

$$l := \widehat{h}_{\text{G}}(0) \leq 1, \quad \max_{x\in[0,L-1]} \widehat{h}_{\text{G}}(x) = 1 \ \text{ and } \ r := \widehat{h}_{\text{G}}(L-1) < 1\,.$$

A user has to choose two parameters:

- $l \in (0, 1]$ which is the desired portion of dark pixels;
- $r \in (0, 1]$ drawing the desired portion of light pixels.

Note that one cannot choose $l = r = 1$. Given $l \in (0, 1]$ and $r \in (0, 1]$, the *shape* of the target histogram reads as

$$\widehat{h}_{\text{G}}(x) = \exp\left(-\frac{(x-\mu)^2}{\sigma}\right), \quad x \in [0, L-1], \quad \text{for}$$
$$\mu = \frac{-(L-1)(\ln l - \sqrt{\ln l\,\ln r})}{\ln r - \ln l}, \quad \sigma = \frac{(L-1)^2(\sqrt{-\ln l} - \sqrt{-\ln r})^2}{(\ln r - \ln l)^2}. \tag{27}$$

Finally the target histogram $\widehat{h}$ is normalized according to the number n of pixels in the image:

$$\widehat{h}(x) = \frac{n\,\widehat{h}_{\text{G}}(x)}{\sum_{x=0}^{L-1} \widehat{h}_{\text{G}}(x)} \quad \forall\, x \in \{0, \cdots, L-1\}.$$

Whenever (27) is used, we shall write $\widehat{h}_{\text{G}}$ for $\widehat{h}$.

Remark 7. *If the input RGB image w has no pixel values on an interval $[0, L_0]$ for some $L_0 \geq 1$ one has to perform the hue-preserving stretching in* (5). *The target histogram is chosen based on the stretched histogram and the enhanced image is computed from the stretched image; see Fig. 16.*

With this cautionary remark, we can explain how to choose good target histograms using (27). The input intensity histogram, after stretching if necessary, is denoted by h_f.

Remark 8. *The choice of the parameters (l, r) to build $\widehat{h}_{\text{G}}$ in* (27) *depends on the input intensity histogram h_f and on the enhancement task. E.g., $(l, r) = (1, 0.99)$ leads to HE.*

(i) Function $\widehat{h}_{\text{G}}$ can be easily adapted to all images whose histogram h_f is roughly unimodal – see the original images in Figs. 6, 7, 9, 10, 11, 13, 14 and 16.
If the pixel values are mainly in the middle of the interval $[0, L-1]$ and decay at the ends (see Figs. 7, 9 and 16), a good enhancement can be done with $l \gtrapprox r \in [0.1, 0.2]$. When h_f rapidly decays towards $L-1$, one should choose $r \in (0, 0.1]$ (see Figs. 6, 10, 11, 13 and 16). The stronger this decay, the smaller the value of r should be selected (e.g. in Fig. 11, $r = 10^{-4}$.)
A too large r should entail artifacts typical for HE.
If most of the pixel have small values (underexposed images, see Figs. 6, 10, 11 and 13), it is reasonable to select $l \in [0.8, 1]$. The higher the concentration near 0, the larger the value of $l \lessapprox 1$ should be taken.

(ii) For images with important very dark and very bright areas, function (27) *should not work well. Then a good option is to take a mixed target histogram*

$$\widehat{h}_{\text{mix}} := \frac{1}{2}(h_f + \widehat{h}_{\text{G}}) \qquad (28)$$

where the parameters (l, r) for $\widehat{h}_{\text{G}}$ are selected following the rules in (i). For example, see Figs. 8, 12 and 15.

This remark is illustrated in Fig. 8.

B. Enhancement Tests

We present some results from a large series of test images with the goal to improve the visual quality. The enhanced image should seem *natural* and an observer should not suspect that it is a post-processing result.

We compare our Multiplicative algorithm 4 (×) with the Naik-Murthey algorithm 2 (NM) and the Additive algorithm 5 (+). The HS in these algorithms is done by Algorithm 1. The histogram of the original intensity image and the target histograms are depicted beneath the images. The percentage of pixels having a gamut problem in Alg. 4 (×), Alg. 5 (+) and Alg. 2 (NM) is contained in Table I. Further we provide comparison results with

- the fast implementation of ACE by [14] available online at `http://demo.ipol.im/demo/g_ace/`, and
- the perceptual color enhancement through variational methods in [7] and [8].

ACE has one main parameter, the enhancement strength α whose default value $\alpha = 0.5$ is often a good choice. For the two perceptual enhancement methods [7] and [8], the authors gave us their codes and helped us to tune the parameters.

We present the results for images with different defects. The parameter values for all methods are given in the captions, as well as the image credits. The original images in Figs. 6, 7, 8, 10, 11, 13, 12 and 16 are photos taken by the authors who wanted to improve them. For all these images, we do not have "ground truth". For Fig. 17 we shot an underexposed and a better "example" image which enabled us to compare with the perceptual histogram-based method in [10].

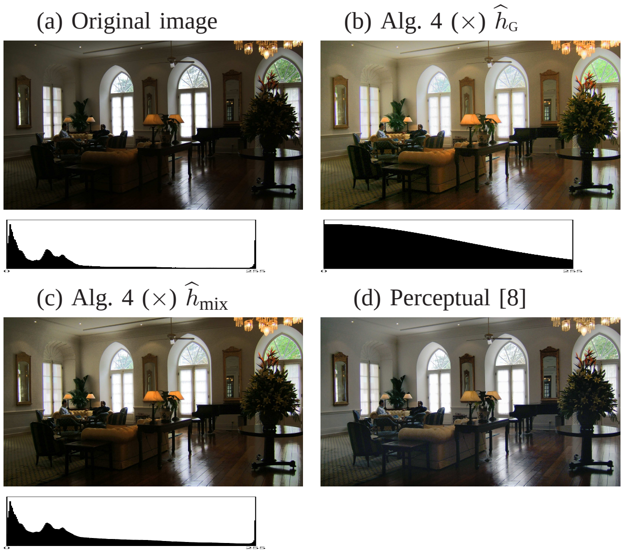
(a) Original image
(b) Alg. 4 (×) $\widehat{h}_{\text{G}}$
(c) Alg. 4 (×) $\widehat{h}_{\text{mix}}$
(d) Perceptual [8]

Fig. 8. (a) Image *club* (1800 × 3200). Enhancement using our Multiplicative algorithm with: (b) $\widehat{h}_{\text{G}}$ for $(l, r) = (1, 0.2)$; (c) $\widehat{h}_{\text{mix}}$ by (28) for $\widehat{h}_{\text{G}}$ as in (b). (d) Enhancement by the variational method in [8].

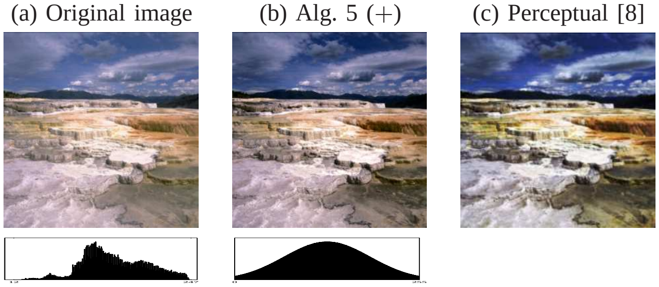
(a) Original image
(b) Alg. 5 (+)
(c) Perceptual [8]

Fig. 9. (a) Image *islanda* (courtesy of P. Greenspun) of size 294×293, and plot of h_f. Enhancement results: (b) Additive algorithm with $\widehat{h}_{\text{G}}$ for $(l, r) = (0.1, 0.1)$, see (27); (c) Perceptual variational method [8] with Michelson's contrast function and default parameters (courtesy of the authors of [8]).

Fig. 8 illustrates Remark 8. The image *club* in (a) is underexposed and its histogram h_f does not obey Remark 8(i). The result in (b) is obtained with a Gaussian target histogram $\widehat{h}_{\text{G}}$ for parameters following (i). In (c) we use a mixed target histogram $\widehat{h}_{\text{mix}}$ as proposed in (28). This image better shows the ambience of the club. The perceptual method [8] in (d) gives a colder color palette.

Two tests with the image *islanda* are shown in Fig. 9. The original in (a) is a rather light image. The Multiplicative, the Additive and the NM algorithms with Gaussian target histograms produce quite similar results, which confirms our discussion in Subsection IV-B. Only the issue of our Additive algorithm is shown in (b). The perceptual method [8] and the ACE perform similarly and give a nice, different color content of the image. We depict the result by [8] in (c).

The photo *boy-on-stones* in Fig. 10(a) was taken in a very sunny day. Due to camera corrections, the picture appears underexposed. Our Multiplicative algorithm gives a realistic result shown in (b). In particular, observe the reflectance of the sunlight on the stones. The NM algorithm yields a grayish result (c). The Additive algorithm (not shown) gives a slightly better enhancement than the NM algorithm which confirms

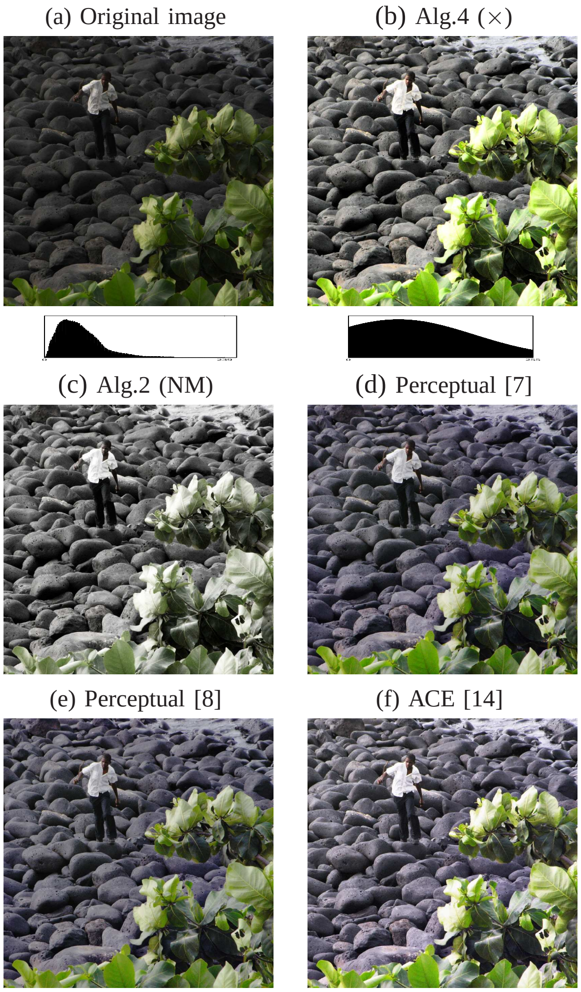

Fig. 10. (a) Image *boy-on-stones* (800×800) and plot of h_f. Enhancement results: (b) Multiplicative algorithm with $\widehat{h}_{\mathrm{G}}$ for $(l, r) = (0.8, 0.2)$; (c) Naik-Murthy algorithm with the same $\widehat{h}_{\mathrm{G}}$; (d) Perceptual variational method [7] with data-fitting parameter $\gamma = 0.2$; (e) Perceptual variational method [8] with a symmetric contrast function and slope parameter 10; (f) ACE, $\alpha = 5$.

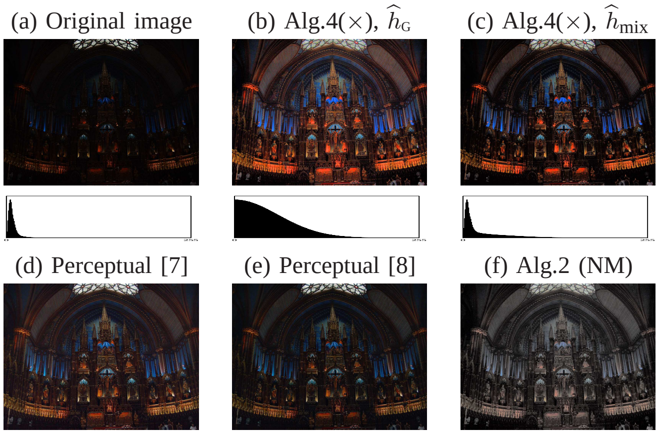
(a) Original image
(b) Alg.4(×), $\widehat{h}_{\mathrm{G}}$
(c) Alg.4(×), $\widehat{h}_{\mathrm{mix}}$
(d) Perceptual [7]
(e) Perceptual [8]
(f) Alg.2 (NM)

Fig. 11. (a) Image *cathedral* (768×1024) and plot of h_f. Enhancement results: (b) Multiplicative algorithm with $\widehat{h}_{\mathrm{G}}$ for $(l, r) = (1, 10^{-4})$; (c) The same algorithm for $\widehat{h}_{\mathrm{mix}}$ in Remark 8(ii) with $\widehat{h}_{\mathrm{G}}$ in (b); (d) Perceptual variational method [7], default parameters; (e) Perceptual variational method [8] with Michelson's contrast function; (f) NM algorithm with $\widehat{h}_{\mathrm{G}}$ in (b).

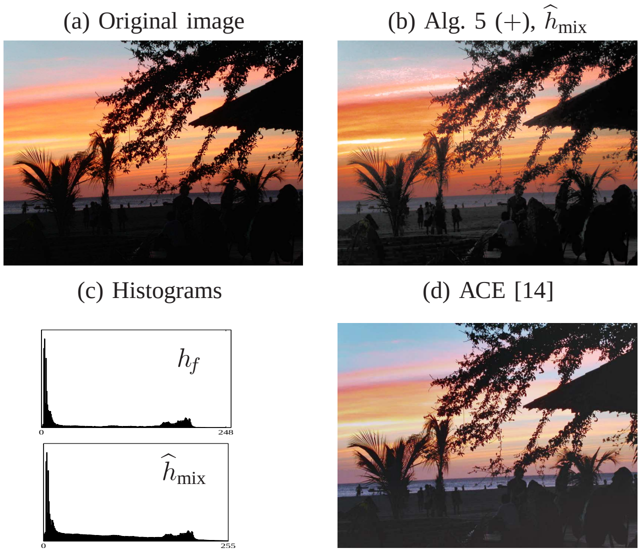
(a) Original image
(b) Alg. 5 (+), $\widehat{h}_{\mathrm{mix}}$
(c) Histograms
(d) ACE [14]
h_f
0
248
$\widehat{h}_{\mathrm{mix}}$
0
255

Fig. 12. (a) Image *Jericoacoara* (886×1181). Enhancement results: (b) Additive algorithm with mixed target histogram $\widehat{h}_{\mathrm{mix}}$ for $(l, r) = (1, 0.1)$; (c) Histograms of the input and the target intensities; (d) ACE for $\alpha = 3$.

our findings in Subsection IV-B. The perceptional variational algorithms [7] in (d) and [8] in (e), as well as the ACE in (f), shift the colors towards blue; observe the stones.

The *cathedral* photo in Fig. 11(a) is much too dark. The result of our Multiplicative algorithm in (b) is quite colorful. The same algorithm for the mixed target histogram (28) gives in (c) a darker and still colorful image. The results of [7] in (d) and [8] in (c) have a darker color palette. The NM algorithm produces a nearly gray value image shown in (f). All results give a different atmosphere.

The photo taken in *Jericoacoara*, Fig. 12(a), has very dark and also some quite clear areas; see h_f in (c). By Remark 8(ii), we use a mixed target histogram $\widehat{h}_{\mathrm{mix}}$. The original has lots of JPEG artifacts so we prefer our Additive algorithm (see Remark 6). The result in (b) is convincing and the details in the dark are clarified. For the ACE in (d) we use a small enhancement, $\alpha = 3$, in order to limit the false color shift.

The *orchid* image in Fig. 13(a) has a bad flashlight effect. This artifact is removed by all tested methods and the background of the scene is clear. Our Multiplicative algorithm gives a realistic colorful result, see (b). As in Fig. 6, our Additive algorithm produces a rather pale image (c) while the issue of the NM algorithm in (d) is too gray. The images obtained by [7] in (e) and by the ACE in (f) exhibit color shifts (see the green leaves on the right and the grass on the bottom left).

The *frog* image in Fig. 14(a) has an intensity histogram between (i) and (ii) in Remark 8. Indeed, both recipes gave similarly good results. The result with $\widehat{h}_{\mathrm{G}}$ is shown in (b). For the ACE in (c) we select a small $\alpha = 3$ limit the color shift.

The *ferrari* image in Fig. 15(a) has very dark and very bright areas. Using Remark 8 (ii), we take a mixed target histogram. Our Multiplicative algorithm gives a realistic image shown in (b) with vivid colors that fit the typical red of the brand. The variational methods [7] in (c) and [8] in (d) outperform the ACE (result not shown).

The image *fields* in Fig. 16(a) was taken trough an aircraft porthole. It has no pixels with values in $[0, 109]$. By Remark

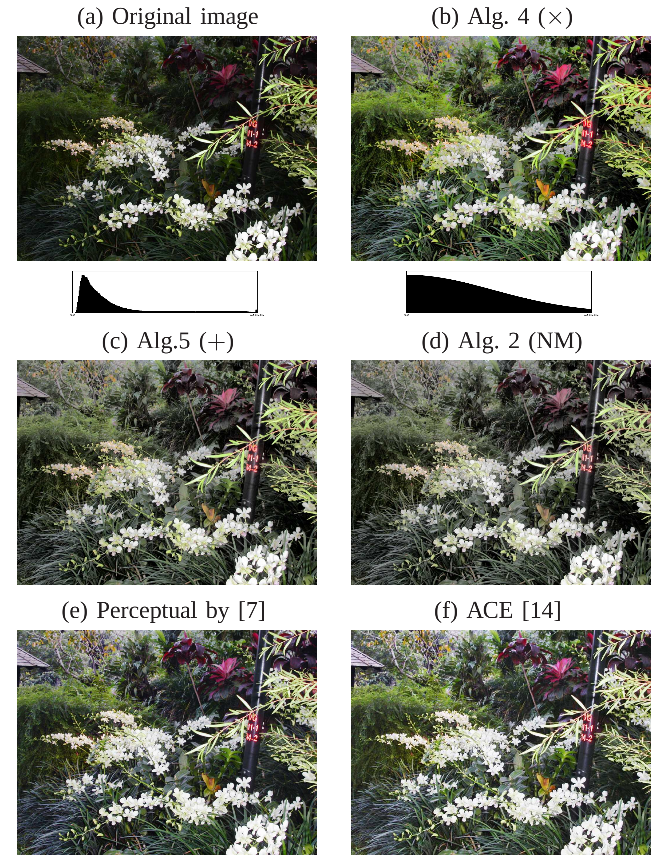

(a) Original image (b) Alg. 4 (×) (c) Alg.5 (+) (d) Alg. 2 (NM) (e) Perceptual by [7] (f) ACE [14]

Fig. 13. (a) Image *orchid* (768×1024) with a bad flashlight effect. Enhancement results: (b) Multiplicative algorithm with $\widehat{h}_{\text{G}}$ for $(l, r) = (1, 0.1)$; (c) Additive algorithm for the same target histogram; (d) NM algorithm [18] for the same target histogram; (e) Perceptual variational method [7] for $\gamma = 0.2$; (f) ACE [14], default parameter.

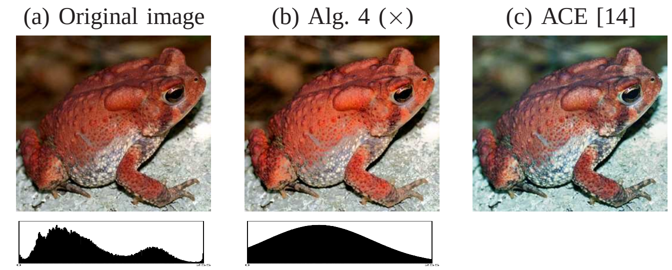

(a) Original image (b) Alg. 4 (×) (c) ACE [14]

Fig. 14. (a) Image *frog*, 332×300 (credits: John D. Willson, USGS Amphibian Research and Monitoring Initiative). Enhancement results: (b) Multiplicative algorithm with $\widehat{h}_{\text{G}}$ for $(l, r) = (0.4, 0.1)$; (c) ACE for $\alpha = 3$.

3, we use in (b) the global hue-preserving stretching. Its further enhancements using our Multiplicative and Additive algorithms give visually the same results, so only the first one is shown in (c). For the ACE in (d) we take $\alpha = 8$ in order to obtain an enhancement strength similar to (c). The JPEG blue artifacts are stronger in (d) compared to (c).

Fig. 17 (a) and (b) show an underexposed and a better exposed "example" image of the same scene *flag*. In [10] the authors propose an algorithm for the color transfer between images (usually of different scenes). Using this algorithm we transferred the colors from the example image (b) to the underexposed one (a). The result in (c) is close to the example

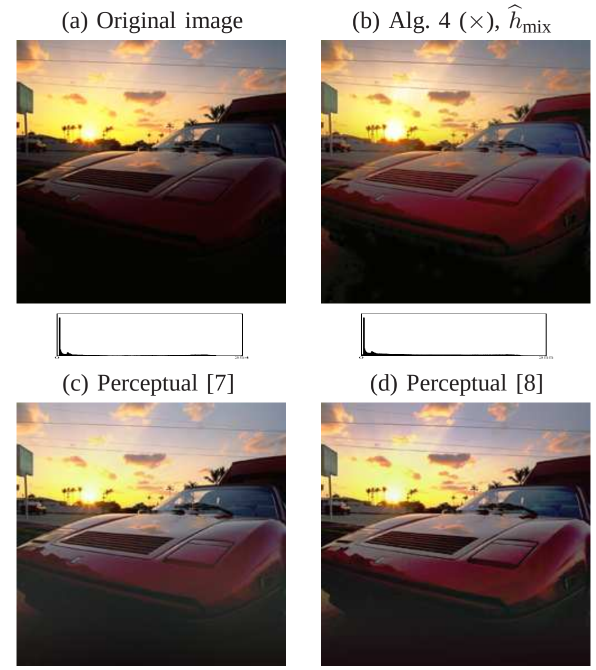

(a) Original image (b) Alg. 4 (×), $\widehat{h}_{\text{mix}}$ (c) Perceptual [7] (d) Perceptual [8]

Fig. 15. (a) Image *ferrari* (courtesy of P. Greenspun) of size 235×240 and histogram of its intensity channel.. Enhancement results: (b) Multiplicative algorithm with mixed target histogram for $(l, r) = (1, 0.1)$; (c) Perceptual variational method [7] with default parameters (courtesy of the authors); (d) Perceptual variational method [8] with Michelson's contrast function and default parameters (courtesy of the authors).

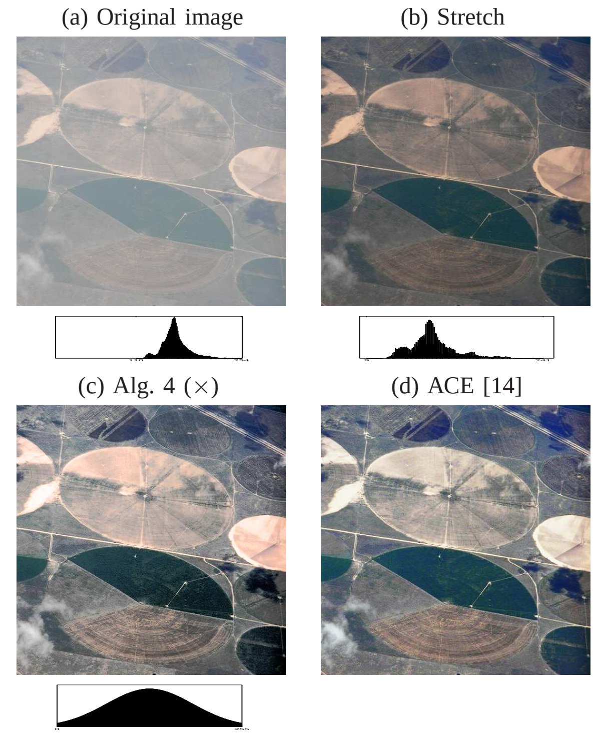

(a) Original image (b) Stretch (c) Alg. 4 (×) (d) ACE [14]

Fig. 16. (a) Image *fields* (512×512) and histogram of its intensity. Enhancement results: (b) Global affine stretching (Remark 3) and intensity histogram; (c) Multiplicative algorithm applied to (b) with Gaussian target histogram for $(l, r) = (0.1, 0.1)$; (d) ACE for $\alpha = 8$ applied to (a).

image	$\sharp\mathcal{U}(1)$	$\sharp\mathcal{U}(0)$	$\sharp\mathcal{L}(0)$	$\sharp\mathcal{V}$
bungalow $\widehat{h}_{\mathrm{G}}$	1.90	0.94	0	98.15
islanda $\widehat{h}_{\mathrm{G}}$	0.89	0.85	0.94	2.93
club $\widehat{h}_{\mathrm{G}}$	0.98	0.23	0.67	94.61
club $\widehat{h}_{\mathrm{mix}}$	0.33	0.15	1.39	92.61
boy-on-stones ($\widehat{h}_{\mathrm{G}}$)	4.76	2.40	0.54	94.15
cathedral ($\widehat{h}_{\mathrm{G}}$)	1.04	0.00	1.38	95.71
Jericoacoara ($\widehat{h}_{\mathrm{mix}}$)	5.98	5.71	0.40	68.26
orchid ($\widehat{h}_{\mathrm{G}}$)	0.21	0.10	1.85	87.93
frog ($\widehat{h}_{\mathrm{G}}$)	0.09	0.08	6.79	80.04
ferrari ($\widehat{h}_{\mathrm{mix}}$)	4.40	4.22	0.30	60.7
fields ($\widehat{h}_{\mathrm{G}}$)	4.61	2.99	2.06	89.16

TABLE I
Percentage of pixels requiring an upper or lower gamut correction. For our Algorithms 4 (×) and 5 (+) the numbers $\sharp\mathcal{U}(1)$, resp., $\sharp\mathcal{U}(0)$, $\sharp\mathcal{L}(0)$ are very small in all tests; this is not the case for $\sharp\mathcal{V}$ in the NM algorithm.

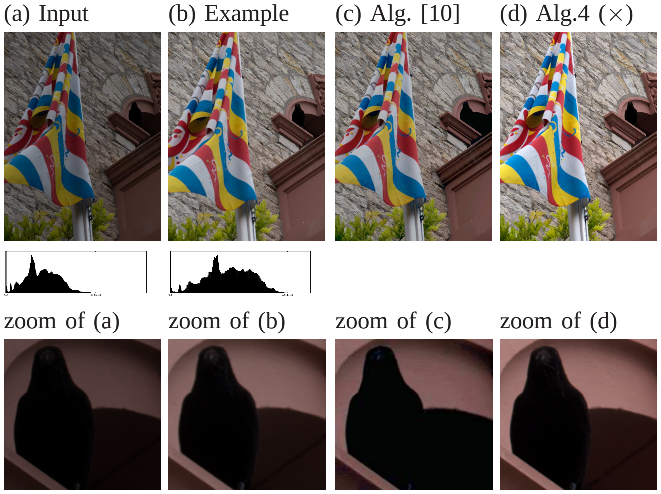
(a) Input (b) Example (c) Alg. [10] (d) Alg.4 (×)

zoom of (a) zoom of (b) zoom of (c) zoom of (d)

Fig. 17. (a) Input underexposed image *flag* (1500 × 1125) and (b) example better-exposed *flag* together with the histograms of their intensities. Enhancement results: (c) the color transfer method [10] and (d) our Multiplicative algorithm with the example target intensity histogram in (b).

image. We have applied our Multiplicative algorithm to image (a) using the intensity histogram of (b). The result, shown in (d), is less dull than the example (b). The third row in Fig. 17 depicts a zoom into the area with the raven (right middle). One observes that the bird is fused with part of the background in (c), whereas it is distinguishable in (b) and (d).

VI. Conclusions and future work

This work provides the first comprehensive and rigorous presentation of the wide family of histogram specification based affine color assignment models. We have proposed a fast hue and range preserving algorithm. We analyzed the performances of this algorithm and two of its important instances as well as the gamut preserving method in [18].

Many open questions have been raised that we want to answer in our future research. Since our algorithms are fast, extensions to video should be envisaged. We are aware of the broad literature on color enhancement taking both global and local neighborhood of pixels into account see, e.g., [6], [7], [8], [13], [36]. It will be interesting to incorporate such information into our framework. Moreover, we want to take into account other important properties of the human visual system.

VII. Appendix

Proof of Proposition 1: A pixel $i \in \mathbb{I}_n$ in (15) has an upper gamut problem if

$$\frac{\lambda\widehat{f}[i]+(1-\lambda)f[i]}{f[i]}M[i]+(1-\lambda)(\widehat{f}[i]-f[i])>L-1. \tag{29}$$

The upper bound follows from the choice of $\widehat{w}_c[i]$, $c \in \{r, g, b\}$ in (12). We focus the lower bound. First we see that (29) implies $\widehat{f}[i] \geq f[i]$, since in case $\widehat{f}[i] < f[i]$ we would get by replacing $\widehat{f}[i]$ by $f[i]$ in the denominator of the quotient and the second summand in (29) the contradiction $M[i] > L-1$. Since $M[i]-f[i] > 0$ the lower bound holds true if and only if

$$\begin{aligned}(L-1-\widehat{f}[i])(w_c[i]-f[i])+\widehat{f}[i](M[i]-f[i]) &\geq 0,\\ (L-1-\widehat{f}[i])w_c[i]-(L-1)f[i]+\widehat{f}[i]M[i] &\geq 0\end{aligned}$$

which is clearly fulfilled if

$$\widehat{f}[i]M[i]-(L-1)f[i] \geq 0. \tag{30}$$

By (29) we have

$$\begin{aligned}&\widehat{f}[i]M[i]-(L-1)f[i]\\ &> \widehat{f}[i]M[i]-\left(\lambda\widehat{f}[i]+(1-\lambda)f[i]\right)(M[i]-f[i])-\widehat{f}[i]f[i]\\ &= \left(\widehat{f}[i]-(\lambda\widehat{f}[i]+(1-\lambda)f[i])\right)(M[i]-f[i]).\end{aligned}$$

By $\widehat{f}[i] \geq f[i]$ the first factor on the right-hand side is ≥ 0 the second one is > 0. Thus, (30) is satisfied. □

Proof of Proposition 2: A pixel $i \in \mathbb{I}_n$ in (15) has a lower gamut problem if

$$\frac{\lambda\widehat{f}[i]+(1-\lambda)f[i]}{f[i]}m[i]+(1-\lambda)(\widehat{f}[i]-f[i])<0. \tag{31}$$

The lower bound is clear from the construction of $w_c[i]$ in (14). We show the upper bound. Developing (14) yields

$$\begin{aligned}\widehat{w}_c[i] &= \frac{\widehat{f}[i]w_c[i]-\widehat{f}[i]\,f[i]+\widehat{f}[i]\,f[i]-\widehat{f}[i]\,m[i]}{f[i]-m[i]}\\ &= \frac{\widehat{f}[i]}{f[i]-m[i]}\,(w_c[i]-m[i]), \quad c \in \{r, g, b\}.\end{aligned} \tag{32}$$

Using (31), one has

$$\widehat{f}[i]\,\frac{\lambda m[i]+(1-\lambda)f[i]}{f[i]}+(1-\lambda)(m[i]-f[i])<0$$

and hence

$$\widehat{f}[i] < \frac{(1-\lambda)f[i]}{\lambda m[i]+(1-\lambda)f[i]}(f[i]-m[i]) < f[i]-m[i].$$

Thus, since $0 < w_c[i]-m[i] < L-1$, we obtain finally

$$\frac{\widehat{f}[i]}{f[i]-m[i]}(w_c[i]-m[i]) < L-1. \qquad \blacksquare$$

Proof of Proposition 3: Let $0 \leq \lambda_1 < \lambda_2 \leq 1$. In the upper gamut case we always have $\widehat{f}[i] > f[i]$. Then $\lambda_1\widehat{f}[i]+(1-\lambda_1)f[i] < \lambda_2\widehat{f}[i]+(1-\lambda_2)f[i]$, hence $G_M^{\lambda_1}[i] \leq G_M^{\lambda_2}[i]$ and $\mathcal{U}(\lambda_1) \subseteq \mathcal{U}(\lambda_2)$. Similarly, since $\widehat{f}[i] < f[i]$ in the lower gamut case, $\lambda_1\widehat{f}[i]+(1-\lambda_1)f[i] > \lambda_2\widehat{f}[i]+(1-\lambda_2)f[i]$ so that $G_m^{\lambda_1}[i] \geq G_M^{\lambda_2}[i]$ and hence $\mathcal{L}(\lambda_1) \supseteq \mathcal{L}(\lambda_2)$. □

Proof of Proposition 4: Let $i \in \mathbb{I}_n \setminus \{\mathcal{U}(1) \cup \mathcal{L}(0)\}$. Then $\widehat{w}_c^{\times}[i]$ is given by (20)(i) and since $\mathcal{U}(0) \subseteq \mathcal{U}(1)$, the value $\widehat{w}_c^{+}[i]$ is given by (21)(i). Consequently,

$$\widetilde{w}_c[i] = \lambda \frac{\widehat{f}[i]}{f[i]} \left(w_c[i] - f[i]\right) + (1-\lambda)(w_c[i] - f[i]) + \widehat{f}[i] = \widehat{w}_c[i],$$

where the last equality follows by $\mathcal{U}(\lambda) \subseteq \mathcal{U}(1)$ and Algorithm 3(i).

Let $i \in \mathcal{U}(0)$. Then $\widehat{w}_c^{+}[i]$ is given by (21)(ii) and since $\mathcal{U}(0) \subseteq \mathcal{U}(1)$, $\widehat{w}_c^{\times}[i]$ is given by (20)(ii). We have $\widehat{w}_c^{+}[i] = \widehat{w}_c^{\times}[i]$ which shows by $\mathcal{U}(0) \subseteq \mathcal{U}(\lambda)$ that $\widetilde{w}_c[i] = \widehat{w}[i]$. □

Proof of Proposition 5: By (22) we have $S(w[i]) = 1 - \frac{m[i]}{f[i]}$, or equivalently, $f[i] - m[i] = f[i]\, S(w[i])$. Algorithm 3 computes

$$\widehat{w}_c[i] = d[i](w_c[i] - f[i]) + \widehat{f}[i], \tag{33}$$

for

$$d[i] = \begin{cases} \lambda \frac{\widehat{f}[i]}{f[i]} + (1-\lambda) & \text{if } i \in \mathbb{I}_n \setminus \{\mathcal{U}(\lambda) \cup \mathcal{L}(\lambda)\}, \\ \frac{L-1-\widehat{f}[i]}{M[i]-f[i]} & \text{if } i \in \mathcal{U}(\lambda), \\ \frac{\widehat{f}[i]}{f[i]\, S(w[i])} & \text{if } i \in \mathcal{L}(\lambda). \end{cases}$$

Since $d[i] > 0$ in all cases, we have

$$\begin{aligned} S(\widehat{w}[i]) &= 1 - \frac{1}{\widehat{f}[i]} \Big(d[i] \big(\min\{w_r[i] w_g[i], w_b[i]\} - f[i] \big) + \widehat{f}[i] \Big) \\ &= 1 - \frac{f[i]}{\widehat{f}[i]} d[i] \frac{\min\{w_r[i], w_g[i], w_b[i]\}}{f[i]} + \frac{f[i]}{\widehat{f}[i]}\, d[i] - 1 \\ &= S(w[i]) \frac{f[i]}{\widehat{f}[i]} d[i]\,. \end{aligned} \tag{34}$$

Inserting the above values $d[i]$ into (34) finishes the proof. □

Proof of Proposition 6: The case $\frac{\widehat{f}[i]}{f[i]} \leq 1$ follows just as a special case of Proposition 5(i) for $\lambda = 1$. Let $\widehat{f}[i] > f[i]$. Then case (ii) in Algorithm 2 can be rewritten as (33) for $d[i] := \frac{L-1-\widehat{f}[i]}{L-1-f[i]}$. Combining this with (34) we are done. □

Acknowledgement: The authors thank M. Bertalmio, E. Provenzi and N. Papadakis for providing their codes corresponding to [7], [8] and [10] and for the discussion. We want to thank the anonymous reviewers for their constructive remarks.

References

[1] R. S. Berns, *Billmeyer and Saltzman's Principles of Color Technology*, Willey & Sons. Roy S., Ca, 3 edition, 2000.

[2] C. Solomon and T. Breckon, *Fundamentals of Digital Image Processing. A Practical Approach with Examples in Matlab*, John Wiley & Sons, UK, 1st edition, 2011.

[3] T. Gevers and A. Smeulders, "Color-based object recognition", *Pattern Recognition*, vol. 32, 1999.

[4] A. C. Bovik, *Handbook of Image and Video Processing (Communications, Networking and Multimedia)*, Academic Press, Orlando, 2005.

[5] R. Gonzalez and R. Woods, *Digital Image Processing*, NJ: Pentice-Hall, 3rd edition, 2007.

[6] G. Sapiro, and V. Caselles, "Histogram Modification via Differential Equations", *J. Differ. Equations*, vol. 135, no. 2, pp. 238–268, 1997.

[7] M. Bertalmío, V. Caselles, E. Provenzi, and A. Rizzi, "Perceptual color correction through variational techniques", *IEEE Trans. Image Process.*, vol. 16, no. 4, pp. 1058–1072, 2007.

[8] R. Palma-Amestoy, E. Provenzi, M. Bertalmío and V. Caselles, "A perceptually inspired variational framework for color enhancement", *IEEE Trans. Pattern Anal. Mach. Intell.*, vol. 31, no. 3, pp. 458–474, 2009.

[9] E. Provenzi, *Perceptual color correction: A variational perspective*, pp. 109–119, Lect. Notes Comput. Sc. 5646. Springer, 2009.

[10] N. Papadakis, E. Provenzi, and V. Caselles, "A variational model for histogram transfer of color images", *IEEE Trans. Image Process.*, vol. 30, no. 6, pp. 1682–1695, 2011.

[11] E. H. Land, "The Retinex Theory of Color Vision", *Scientific American*, vol. 237, no. 6, 1977.

[12] C. Gatta, A. Rizzi, and D. Marini, "ACE:", in *An automatic color equalization algorithm*. Proceedings: Conference Color in Graphics Image and Vision (CGIV), vol. 5, 2002, pp. 316–320.

[13] A. Rizzi, C. Gatta, and D. Marini, "A new algorithm for unsupervised global and local color correction", *Pattern Recognit. Lett*, vol. 124, 2003.

[14] P. Getreuer, "Automatic color enhancement (ACE) and its fast implementation", *Image Processing On Line*, DOI: 10.5201/ipol.2012.g-ace, vol. 2012, 2012.

[15] M. Bertalmío, V. Caselles, and E. Provenzi, "Issues About Retinex Theory and Contrast Enhancement", *Int. J. Comput. Vis.*, vol. 83, pp. 101–119, 2009.

[16] P. E. Trahanias and A. Venetsanopoulos, "Color image enhancement through 3-D histogram equalization", in *Proc. 15th IAPR Int. Conf. Pattern Recognit*, 1997, vol. 1, pp. 545–548.

[17] J. H. Han, S. Yang, and B. U. Lee, "A novel 3-D color histogram equalization method with uniform 1-D gray scale histogram", *IEEE Trans. Image Process.*, vol. 20, no. 2, pp. 506–512, Feb. 2011.

[18] S. F. Naik and C. A. Murthy, "Hue-preserving color image enhancement without gamut problem", *IEEE Trans. Image Process.*, vol. 12, no. 12, pp. 1591–1598, 2003.

[19] N. Bassiou and C. Kotropoulos, "Color image histogram equalization by absolute discounting back-off", *Computer Vision and Image Understanding*, vol. 107, 2007.

[20] Z. Y. Chen, B. R. Abidi, D. L. Page, and M. A. Abidi, "Gray-Level Grouping (GLG): An automatic method for optimized image contrast enhancementpart i: The basic method", *IEEE Trans. Image Process.*, vol. 15, no. 8, pp. 2290–2302, 2006.

[21] D. Menotti, L. Najman, A. d. Araújo, and J. Facon, "A fast hue-preserving histogram equalization method for color image enhancement using a bayesian framework", in *Proc. 14th Int.Workshop Syst., Signal Image Process. (IWSSIP)*, 2007, pp. 414–417.

[22] D. Menotti, L. Najman, J. Facon, and A. Albuquerque, "Histogram equalization methods for color image contrast enhancement", *Int. J. Comput. Sci. & Inform. Technology* , vol. 4, no. 5, pp. 243–259, 2012.

[23] N. Kong and H. Ibrahim, "Color image enhancement using brightness preserving dynamic histogram equalization", *IEEE Trans. Consum. Electron.*, vol. 54, no. 4, pp. 1962–1967, 2008.

[24] M. Nikolova, "A fast algorithm for exact histogram specification. Simple extension to colour images", Lect. Notes Comput. Sc. 7893, Springer, 2013, pp. 174–185.

[25] T. Arici, S. Dikbas, and Y. Altunbasak, "A histogram modification framework and its application for image contrast enhancement", *IEEE Trans. Image Process.*, vol. 18, no. 9, pp. 1921–1935, 2009.

[26] Q. Wang and R. K. Ward, "Fast image/video contrast enhancement based on weighted thresholded histogram equalization", *IEEE Trans. Consum. Electron.*, vol. 53, no. 2, pp. 757–764, 2007.

[27] D. Sen and P. Sankar, "Automatic exact histogram specification for contrast enhancement and visual system based quantitative evaluation", *IEEE Trans. Image Process.*, vol. 20, no. 5, pp. 1211–1220, 2011.

[28] G. Thomas, "A modified version of van-cittert's iterative deconvolution procedure", *IEEE Trans. Acoust. Speech, Signal Process.*, vol. ASSP-29, pp. 938–939, 1981.

[29] C.-L. Chien and D.-C. Tseng, "Color image enhancement with exact HSI color model", *Int. J. of Innovative Computing, Information and Control*, vol. 7, no. 12, pp. 6691–6710, 2011.

[30] D. Coltuc, P. Bolon, and J.-M. Chassery, "Exact histogram specification", *IEEE Trans. Image Process.*, vol. 15, no. 6, pp. 1143–1152, 2006.

[31] Y. Wan and D. Shi, "Joint exact histogram specification and image enhancement through the wavelet transform", *IEEE Trans. Image Process.*, vol. 16, no. 9, pp. 2245–2250, 2007.

[32] M. Nikolova and G. Steidl, "Fast sorting algorithm for exact histogram specification", Preprint hal-00870501, 2013.

[33] M. Nikolova, Y.-W. Wen, and R. Chan, "Exact histogram specification for digital images using a variational approach", *J. Math. Imaging and Vision*, vol. 46, no. 3, pp. 309–325, 2013.

[34] C. C. Yang and J. J. Rodriguez, "Efficient luminance and saturation processing techniques for bypassing color coordinate transformations", in *Proc. IEEE Int. Conf. on Systems, Man, and Cybernetics*, 1995, vol. 1, pp. 667–672.

[35] C. C. Yang and J. J. Rodriguez, “Saturation clipping in the lhs and yiq color spaces”, in *Proc. IS&T/SPIE Int. Symp. Electronic Imaging: Science & Technology Color Imaging: Device-Independent Color, Color Hard Copy, and Graphic Arts*, 1996, vol. 1.

[36] J.-Y. Kim and L.S. Kim, “An advanced contrast enhancement using partially overlapped sub-block histogram equalization”, *IEEE Trans. Circ. Sys. Video*, vol. 11, no. 4, pp. 475–484, 2001.

Gabriele Steidl received her PhD and Habilitation in Mathematics from the University of Rostock, Germany, in 1988 and 1991, respectively. From 1993 to 1996, she held a position as assistant professor of Applied Mathematics at the University of Darmstadt, Germany. From 1996 to 2010, she was full professor at the Department of Mathematics and Computer Science, University of Mannheim, Germany. Since 2011, she is Professor at the Department of Mathematics at the University of Kaiserslautern, Germany. She was a visiting researcher at the University of Debrecen (Hungary), the University of Zrich (Switzerland), the Banach Center Warsaw (Poland), the ENS Cachan and the University Paris Est (France). Her research interests include applied and computational harmonic analysis and convex analysis with applications in image processing.

Mila Nikolova received the Ph.D. degree from the Université de Paris-Sud, France, in 1995. She got a Habilitation to direct research in 2006. Currently, she is Research Director with the National Center for Scientific Research (CNRS), France. She performs herduty as a full-time researcher at CMLA (Centre de Mathématiques et de Leurs Applications), Department of Mathematics, ENS Cachan, France. Her research interests are in mathematical Image and signal reconstruction, Inverse problems, Regularization and variational methods and the properties of their solutions, Scientific computing.